Rapid Communications

Subthreshold laser jetting via flow-focusing in laser-induced forward transfer

Emre Turkoz,[1] SeungYeon Kang,[1] Luc Deike,[1,2] and Craig B. Arnold[1,*]
[1]*Department of Mechanical and Aerospace Engineering, Princeton University, Princeton, New Jersey 08544, USA*
[2]*Princeton Environmental Institute, Princeton University, Princeton, New Jersey 08544, USA*

(Received 25 June 2018; published 15 August 2018)

Increasing the printing resolution of drop-on-demand printing and deposition techniques is important for many industrial applications. In this Rapid Communication, we present a technique to minimize the jet size and reduce the laser threshold energy of a variant of the laser-induced forward transfer (LIFT) process called blister-actuated LIFT. We fabricate micrometer-sized holes onto the solid polyimide thin-film substrate which hosts the donor liquid ink film to be printed. Due to the micrometer size of the holes, surface tension effects are enhanced, a meniscus is formed at the air-ink interface, and the resulting focused jets are thinner and faster than regular jets.

DOI: 10.1103/PhysRevFluids.3.082201

Flow-focusing has been used in microfluidics to generate droplets that are smaller than the size of the orifice structure used to form jets [1,2]. It has recently been shown that it is possible to generate very thin, fast jets and eject smaller droplets from capillary tubes by introducing a pressure impulse using a laser pulse [3,4] or the impact resulting from the free fall of a capillary tube onto a rigid surface [5,6]. In these applications, the meniscus at the air-liquid interface plays a crucial role. The flow-focusing phenomenon is due to the rapid reduction in the effective surface area of the meniscus during the initial phases of the flow [7]. The reducing effective surface area leads to additional acceleration for the jet formation which results in the formation of thinner and faster jets.

The resolution of the jet-based drop-on-demand printing techniques depends on the ejected droplet volume at each deposition step [8]. Laser-induced forward transfer (LIFT) is a technique where a controlled amount of material is transferred from a donor thin film to a receiving substrate by means of a laser pulse [9]. LIFT has been shown to have a superior resolution compared to the conventional ink jet printing technique during the printing of various simple [10] and complex inks [11,12]. This technique has been used in the fabrication of various structures such as graphene oxide films [13], polymeric lenses [14], alkaline- and lithium-based microbatteries [15], and biomaterials such as DNA [16]. In all of these applications, the printing resolution is dictated by the flat ink film thickness, the laser spot size, and the laser energy.

In order to combine the advantages of the flow-focusing and LIFT, we use a LIFT variant called blister-actuated LIFT (BA-LIFT) [17,18] with a structured surface. BA-LIFT is a LIFT technique in which a laser pulse is absorbed by a solid polyimide interfacial layer that forms a rapidly growing blister, where the blister results from the plastic deformation on the polyimide layer [19], as shown in Fig. 1(a). We introduce flow-focusing into the BA-LIFT process by creating holes on top of the polyimide surface to create a meniscus between the ink and the air interface. As shown in Fig. 1(b), a photoresist layer is coated on top of the polyimide layer and patterned to generate the holes. We show in this Rapid Communication that the formed jets are faster and thinner compared to the regular

*cbarnold@princeton.edu

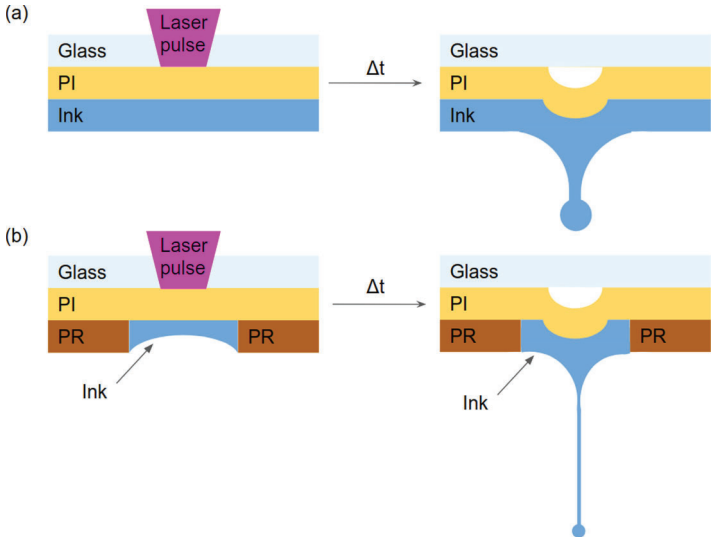

FIG. 1. Schematic of blister-actuated laser-induced forward transfer (BA-LIFT) with and without flow-focusing. (a) The conventional BA-LIFT technique. The laser pulse is absorbed by the polyimide (PI) layer which leads to the rapid formation of a blister. This leads to the deformation of the ink film and jet formation. (b) BA-LIFT with flow-focusing. The ink inside the hole of the photoresist (PR) layer forms a meniscus at the liquid-air interface. The curved interface leads to the flow-focusing with the pressure impulse from the blister.

BA-LIFT jets, and this technique enables the subthreshold jetting which increases the resolution of the BA-LIFT process.

The fabrication of the micrometer-sized holes is performed in a clean room. We first salinize 2.5×2.5 cm glass slides by spin coating adhesion promoter (diluted VM-651, HD Microsystems) at 4000 rpm. Next, the interfacial polyimide layer is formed by spin coating polyimide resin (PI2525, HD Microsystems) at 500 rpm for 10 s, followed by a faster spin at 3000 rpm for 40 s. This yields an approximately 7-μm-thick polyimide film. To complete the imidization process the slides are baked at 160 °C for 20 min, followed by another 20 min at 360 °C. To add the microscale hole structures that can hold the ink, we spin coat photoresist (AZ 4330-RS, Merck KGaA) at 1000 rpm for 40 s on to the polyimide layer, followed by a soft baking step at 110 °C for 60 s. This gives an approximately 7-μm-thick photoresist film on top of the polyimide layer. The photoresist layer was patterned in various dimensions using a high-resolution laser lithography system (DWL 66+, Heidelberg Instruments). As shown in Fig. 2(a), the hole walls are made of the photoresist layer which helps in creating the meniscus structure. The hole and meniscus profiles are measured using confocal microscopy.

The ink [de-ionized water with 0.1 wt. % Triton X-100 surfactant (surface tension $\gamma = 30.4$ mN/m)] is coated by injecting a few drops on the substrate using a syringe. The excessive ink is cleared using a doctor blade. The laser pulse with 355 nm is generated using a frequency-tripled Nd:YVO_4 laser (Coherent AVIA, 20 ns). The laser beam is focused on the polyimide layer with a spot size of approximately 20 μm using a 10× objective [numerical aperture (NA) = 0.25]. The jet formation is captured using a time-resolved imaging setup whose details are presented in our previous study [20].

We investigate the effects of flow-focusing on BA-LIFT using five different laser pulse energies in two differently sized holes. Figure 2(a) presents a three-dimensional (3D) image of a sample of holes on the polyimide surface with an image of the filled and empty holes. An example meniscus profile is given in Fig. 2(b). In this figure, we also plot the profiles of the two different-sized holes used in this study ($R_1 = 45$ μm and $R_2 = 35$ μm). We measure the minimum distance between the hole bottom

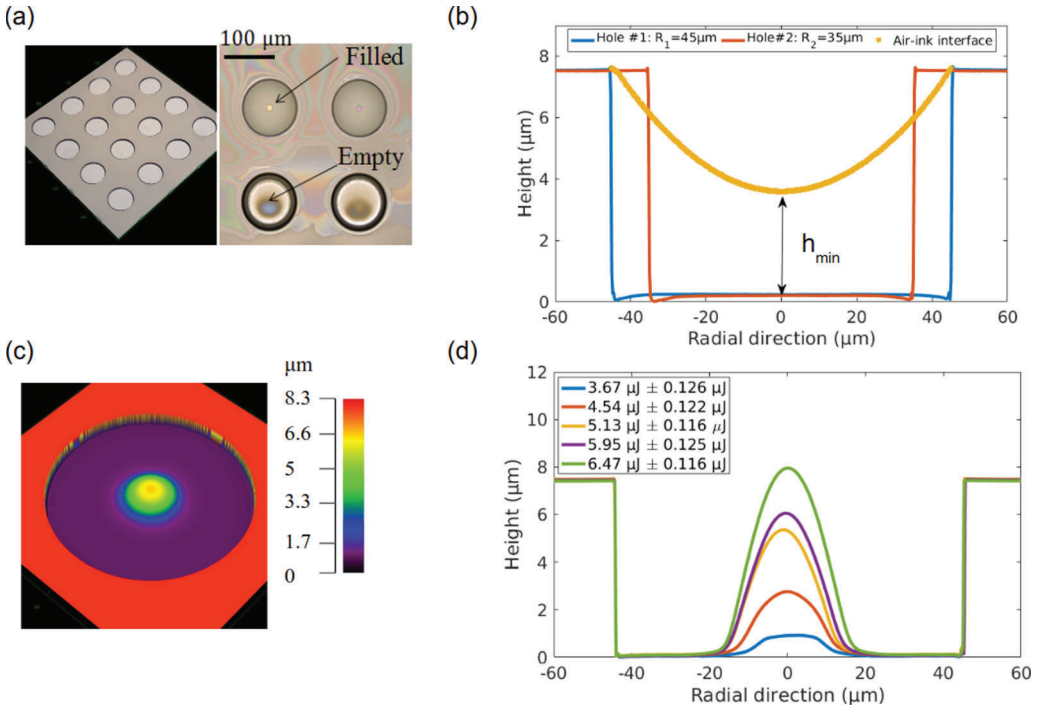

FIG. 2. Profiles of machined holes, blisters generated by the laser pulse, and meniscus on the air-ink interface. (a) A 3D image of the hole pattern fabricated on the polyimide substrate along with the confocal image showing the filled and empty holes together. (b) Profiles of the two types of holes used in this study ($R_1 = 45$ μm and $R_2 = 35$ μm). The ink layer follows a paraboliclike profile with a measured $h_{\min} = 3.8$ μm $\pm$ 0.9 μm value that defines the minimum distance between the hole bottom surface and the air-ink interface. (c) A 3D image and variation in height as a contour plot of a blister generated inside a 45-μm-radius hole. (d) Blister profiles as the result of the five different laser pulse energy levels used in this study. The profiles of the blisters and the holes are measured using confocal microscopy.

surface and the air-ink interface $h_{\min}$ as 3.8 μm $\pm$ 0.9 μm. We evaluate the meniscus angle θ_m using this mean value and the formula $\theta_m = \tan^{-1}[R_1/(h_0 - h_{\min})] = 85.2^\circ$, where $h_0 = 7.5$ μm is the hole depth. This meniscus angle implies the existence of a rather weak meniscus, which we show to be sufficient to create flow-focusing. The meniscus angle value is preserved with the hole radius as long as the Bond number $\mathrm{Bo} = \Delta\rho g R^2/\gamma \approx 0.0004$ stays below 1, where $\Delta\rho$ is the density difference between air and ink, g is the gravity, and R is the hole radius. Figure 2(c) shows an example of a blister generated using a 6.47-μJ laser pulse inside a 45-μm-radius hole overlayed with the contour plot showing the height as a parameter. Figure 2(d) shows the blister profiles measured using confocal microscopy with the five different laser energies. The generated blisters have a Gaussian profile as the laser pulse.

A set of time-resolved images of the regular and focused BA-LIFT jets generated with the same laser pulse energy of 5.95 μJ has been presented in Fig. 3. We show that the focused jets [Fig. 3(b)] look qualitatively different compared to the regular BA-LIFT jets [Fig. 3(a)] as focused jets are thinner and get longer in a given time. The regular BA-LIFT jet shown in Fig. 3(a) is created from a 7.8-μm flat film while the hole depth h_0 for the flow-focusing jet shown in Fig. 3(b) is $h_0 = 7.5$ μm. The focused jet, which is approximately 5 μm thick at 7 μs, has an average value of 145 m/s while the regular jet has an average value of 18 m/s. Figures 3(c) and 3(d) show the examples of single drop ejections from a jet induced from a 8.1-μm flat film and the smaller hole with $R_2 = 35$ μm, respectively. The jet length for the five laser pulse energies and resulting blisters as a function of time is

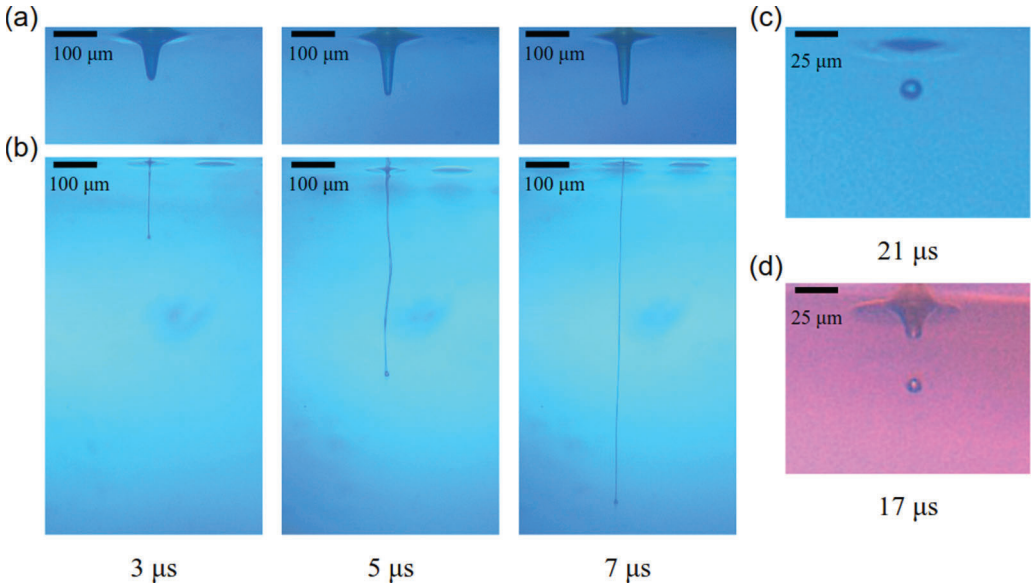

FIG. 3. Examples of time-resolved images of the BA-LIFT process. Jet formation is shown (a) without and (b) with flow-focusing. The flat-film thickness is measured as 7.8 μm, which is very close to the hole depth $h_0 = 7.5$ μm. The laser pulse energy in both cases (a) and (b) is 5.95 μJ. The focused jet has an average velocity of 145 m/s while the regular BA-LIFT jet has an average velocity of 18 m/s. Examples of single drop ejections are shown in (c) from a flat film of 8.1 μm using the laser transfer threshold energy $E_{\text{th}} = 4.15$ μJ and in (d) from the smaller hole ($R_2 = 35$ μm) using $E_{\text{th}} = 3.05$ μJ.

shown in Fig. 4(a) for $t \geqslant 2$ μs. This plot is generated after the postprocessing of 460 time-resolved images corresponding to approximately eight images per time step for each hole and laser pulse energy. We do not plot the values for $t \leqslant 2$ μs because the standard deviations are comparable to the measured average jet length values, and it is therefore not possible to make a good distinction between profiles obtained at different laser pulse energies.

The average jet velocities are obtained by fitting a linear curve [$L_j = V_j(t - t_0)$] onto the data points presented in Fig. 4(a). We note that higher energies lead to longer jets which break up into more droplets and result in a larger deposition volume. Therefore, lower energies that are closer to the threshold energy are more suitable for printing [21]. The average jet velocities are plotted as a function of the laser pulse energy in Fig. 4(b). In this figure, the average jet velocities of focused jets from two holes (H1 and H2) having different radius ($R_1 = 45$ μm and $R_2 = 35$ μm) values are compared with two regular BA-LIFT jets from flat films having different ink thickness (H_f) values (6.6 and 8.1 μm). We see that the jets created from the smaller hole are consistently faster than the jets created from the larger hole at a given energy, and the jet velocity increases with the laser pulse energy, as expected. The reason for the difference between the focused and regular jets is the flow-focusing phenomenon resulting from the meniscus at the air-ink interface. For focused jets, the total acceleration of the jet a_{total} at the initial phases of the flow can be expressed as the sum of the acceleration caused by the rapid blister formation a_b and the acceleration due to flow-focusing a_f, $a_{\text{total}} = a_b + a_f$. The acceleration due to blister formation a_b is a function of laser energy, spot size, ink thickness, and material properties, as explained in our previous studies [21,22]. On the other hand, the acceleration due to flow-focusing a_f can be related to the configuration parameters as $a_f \propto \cos\theta_m / R$, which is derived from the flux conservation around a shrinking effective surface area at the interface during the initial phases of the jet formation [7]. This relation implies that the acceleration due to flow focusing is larger if the ink wets the hole surface more or the radius of the

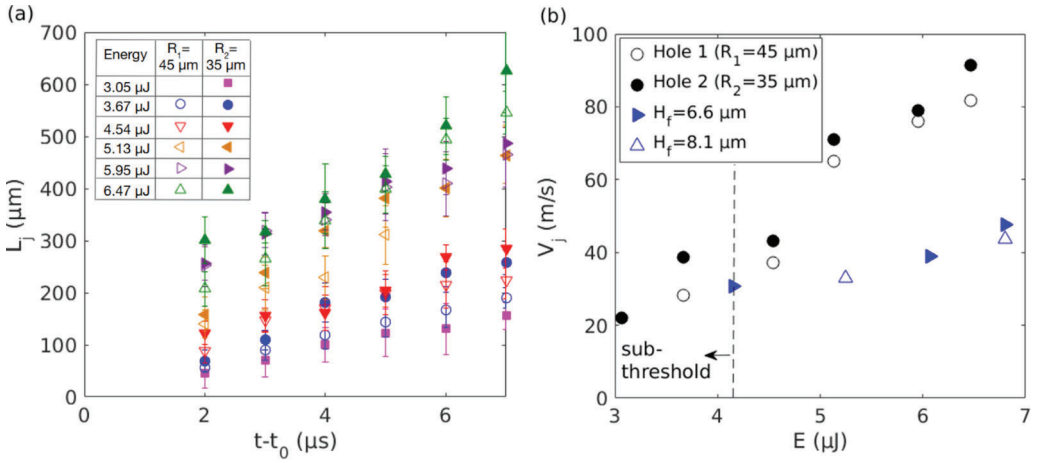

FIG. 4. Analysis of time-resolved imaging results. (a) The jet length L_j as a function of time $t - t_0$, where t_0 is the time when the laser pulse is shot. A higher laser pulse energy and a smaller hole diameter yield faster jets. (b) The change of the average jet velocity V_j as a function of the laser pulse energy E. The open circle (○) markers denote the jet velocities from the larger holes with $R_1 = 45$ μm and the solid circle (●) markers denote the jet velocities for the smaller holes with $R_2 = 35$ μm. The open (△) and solid triangle (▶) markers show the regular BA-LIFT jets induced from flat films with the ink thickness of $H_f = 8.1$ μm and $H_f = 6.6$ μm, respectively. With flow-focusing, it is possible to generate subthreshold jets with energies below 4.15 μJ, which is the laser transfer threshold energy for flat 6.6-μm films.

hole is smaller. Even with a shallow meniscus as in our case, the flow-focusing takes place because the holes have radii of $R_1 = 45$ μm and $R_2 = 35$ μm, as stated above.

Flow-focusing allows jetting and deposition of droplets with lower energies that are not achievable with the flat-film configuration. With flow-focusing, we were able to generate a jet with energies as low as 3.05 μJ, while with the conventional flat-film configuration, we were able to generate a jet with 4.15 μJ for the $H_f = 6.6$ μm thick film and with 5.25 μJ for the $H_f = 8.1$ μm thick film. This subthreshold jetting allows for the creation of jets that results in smaller transfer volumes as the deposited droplet radius R_d also decreases with flow-focusing. When we use laser transfer threshold pulse energy at a given configuration, it is possible to induce jets that result in single droplet deposition. The droplet radius values evaluated from time-resolved images are presented in Table I. As studied before [20,21], the single drops ejected from thin films with the BA-LIFT technique have a radius approximately equal to the film thickness $R_d \approx H_f$. With flow-focusing, we observe that the ejected droplet radius can be as low as 3.8 μm, which is approximately half of the hole depth 7.5 μm. We note that this corresponds to an improvement of 50% in resolution with single drop deposition.

TABLE I. Ejected droplet radius at laser transfer threshold energy E_{th} for each configuration. Flow-focusing configuration holes (holes 1 and 2) have 7.5-μm depth.

Configuration	Average droplet radius	E_{th}
$H_f = 8.1$ μm flat film	$R_d = 9.0 \pm 1.8$ μm	5.25 μJ
$H_f = 6.6$ μm flat film	$R_d = 7.1 \pm 2.1$ μm	4.15 μJ
Hole 1 ($R_1 = 45$ μm)	$R_d = 4.5 \pm 1.0$ μm	3.67 μJ
Hole 2 ($R_2 = 35$ μm)	$R_d = 3.8 \pm 0.6$ μm	3.05 μJ

We show in this Rapid Communications that it is possible to lower the threshold energy required to transfer ink using blister-actuated laser-induced forward transfer by introducing the flow-focusing into the system. Flow-focusing further reduces the jet and the subsequently ejected droplet diameter. In this study, we introduce experiments to include the flow-focusing effect into BA-LIFT. A future study should investigate the experimental parameters affecting the ejected droplet size such as the machined hole diameter, hole depth, and blister size to optimize the technique according to the properties of the ink to be printed. This technique can be extended to other laser-direct write techniques with or without a dynamic release layer that hosts the ink to be printed as long as it is possible to machine micrometer-sized holes that can host the ink to be printed.

This research is supported by the National Science Foundation (NSF) through a Materials Research Science and Engineering Center (MRSEC) program (DMR-1420541).

[1] S. L. Anna, N. Bontoux, and H. A. Stone, Formation of dispersions using flow focusing in microchannels, Appl. Phys. Lett. **82**, 364 (2003).
[2] A. M. Ganán-Calvo and J. M. Gordillo, Perfectly Monodisperse Microbubbling by Capillary Flow Focusing, Phys. Rev. Lett. **87**, 274501 (2001).
[3] Y. Tagawa, N. Oudalov, C. W. Visser, I. R. Peters, D. van der Meer, C. Sun, A. Prosperetti, and D. Lohse, Highly Focused Supersonic Microjets, Phys. Rev. X **2**, 031002 (2012).
[4] P. Delrot, M. A. Modestino, F. Gallaire, D. Psaltis, and C. Moser, Inkjet Printing of Viscous Monodisperse Microdroplets by Laser-induced Flow Focusing, Phys. Rev. Appl. **6**, 024003 (2016).
[5] A. Kiyama, Y. Tagawa, K. Ando, and M. Kameda, Effects of a water hammer and cavitation on jet formation in a test tube, J. Fluid Mech. **787**, 224 (2016).
[6] H. Onuki, Y. Oi, and Y. Tagawa, Microjet Generator for Highly Viscous Fluids, Phys. Rev. Appl. **9**, 014035 (2018).
[7] I. R. Peters, Y. Tagawa, N. Oudalov, C. Sun, A. Prosperetti, D. Lohse, and D. van der Meer, Highly focused supersonic microjets: Numerical simulations, J. Fluid Mech. **719**, 587 (2013).
[8] B. Derby, Inkjet printing of functional and structural materials: Fluid property requirements, feature stability, and resolution, Annu. Rev. Mater. Res. **40**, 395 (2010).
[9] P. Serra and A. Piqué, Introduction to laser-induced transfer and other associated processes, in *Laser Printing of Functional Materials: 3D Microfabrication, Electronics and Biomedicine* (Wiley, Hoboken, NJ, 2018), Chap. 1, p. 3.
[10] J. M. Fernández-Pradas, C. Florian, F. Caballero-Lucas, P. Sopeña, J. L. Morenza, and P. Serra, Laser-induced forward transfer: Propelling liquids with light, Appl. Surf. Sci. **418**, 559 (2016).
[11] P. Delaporte and A.-P. Alloncle, Laser-induced forward transfer: A high resolution additive manufacturing technology, Opt. Laser Technol. **78**, 33 (2016).
[12] M. Makrygianni, A. Millionis, C. Kryou, I. Trantakis, D. Poulikakos, and I. Zergioti, On-demand laser printing of picoliter-sized, highly viscous, adhesive fluids: Beyond inkjet limitations, Adv. Mater. Interfaces 1800440 (2018).
[13] S. Papazoglou, C. Petridis, E. Kymakis, S. Kennou, Y. S. Raptis, S. Chatzandroulis, and I. Zergioti, *In-situ* sequential laser transfer and laser reduction of graphene oxide films, Appl. Phys. Lett. **112**, 183301 (2018).
[14] C. Florian, S. Piazza, A. Diaspro, P. Serra, and M. Duocastella, Direct laser printing of tailored polymeric microlenses, ACS Appl. Mater. Interfaces **8**, 17028 (2016).
[15] C. B. Arnold, P. Serra, and A. Piqué, Laser direct-write techniques for printing of complex materials, MRS Bull. **32**, 23 (2007).
[16] P. Serra, M. Colina, J. M. Fernández-Pradas, L. Sevilla, and J. L. Morenza, Preparation of functional DNA microarrays through laser-induced forward transfer, Appl. Phys. Lett. **85**, 1639 (2004).

[17] N. T. Kattamis, P. E. Purnick, R. Weiss, and C. B. Arnold, Thick film laser induced forward transfer for deposition of thermally and mechanically sensitive materials, Appl. Phys. Lett. **91**, 171120 (2007).

[18] E. Turkoz, R. Fardel, and C. B. Arnold, Advances in blister-actuated laser-induced forward transfer (BA-LIFT), in *Laser Printing of Functional Materials: 3D Microfabrication, Electronics and Biomedicine* (Ref. [9]), Chap. 5, pp. 91–121.

[19] N. T. Kattamis, M. S. Brown, and C. B. Arnold, Finite element analysis of blister formation in laser-induced forward transfer, J. Mater. Res. **26**, 2438 (2011).

[20] E. Turkoz, A. Perazzo, H. Kim, H. A. Stone, and C. B. Arnold, Impulsively Induced Jets from Viscoelastic Films for High-resolution Printing, Phys. Rev. Lett. **120**, 074501 (2018).

[21] M. S. Brown, C. F. Brasz, Y. Ventikos, and C. B. Arnold, Impulsively actuated jets from thin liquid films for high-resolution printing applications, J. Fluid Mech. **709**, 341 (2012).

[22] C. F. Brasz, C. B. Arnold, H. A. Stone, and J. R. Lister, Early-time free-surface flow driven by a deforming boundary, J. Fluid Mech. **767**, 811 (2015).